

An improved model for describing the contrast bolus in perfusion MRI

Vishal Patil^{a)} and Glyn Johnson

Center for Biomedical Imaging, Department of Radiology, New York University School of Medicine,
660 First Avenue, New York, New York 10016

(Received 18 May 2011; revised 10 October 2011; accepted for publication 14 October 2011;
published 9 November 2011)

Purpose: Quantification of perfusion measurements using dynamic, susceptibility-weighted contrast-enhanced (DSC) MRI depends on estimating the size and shape of the tracer bolus. Typically, the bolus is described as a gamma variate function (GV) fitted to the bolus portion of tracer concentration time curve (CTC). However, the last point to fit is arbitrary which can lead to considerable variation in the fitted curve in the presence of noise. In this technical note, we present a model which takes into account recirculation explicitly and fits robustly to the entire CTC in the presence of noise.

Methods: Signal data measurements from ten DSC MRI patients were fitted with our new model and a GV function using four different methods of estimating the end of the bolus. Estimates of the area under the curves (AUC) and first moments (FMs) of the bolus were compared at different noise levels.

Results: The new model gave errors similar to or smaller than those of the most effective methods for fitting a GV.

Conclusions: The single compartment recirculation (SCR) model is the most robust fitting technique with respect to noise both for bias and variability. © 2011 American Association of Physicists in Medicine. [DOI: 10.1118/1.3658570]

Key words: perfusion, bolus, tracer kinetics, recirculation

I. INTRODUCTION

Dynamic, susceptibility-weighted contrast-enhanced (DSC) MRI is a powerful imaging tool for estimation of perfusion parameters such as cerebral blood volume (CBV) and cerebral blood flow (CBF).

When calculating perfusion parameters it is normal to model the concentration time curve (CTC) by an analytic function. Usually, this is a gamma variate function fitted to the first pass portion of the CTC

$$g(t) = A(t - t_0)^\alpha \exp(-(t - t_0)/\beta); \quad t > t_0, \quad (1)$$

where A is a scaling factor, α and β determine the bolus shape, and t_0 is the bolus arrival time.

An alternative CTC model, that we will call the single compartment recirculation (SCR), has also been proposed¹

$$C(t) = g(t) + \kappa \int_0^t g(\tau) d\tau, \quad (2)$$

where κ is a unitless constant less than one (usually around 0.05 for a DSC MRI CTC). The integral term describes recirculating contrast. This fraction is composed of tracer absorbed as the bolus passes through other tissue compartments and released thereafter and of tracer dispersed through the vasculature through mixing.

We believe that the SCR model is preferable to the alternative gamma variate (GV) model for a number of reasons. First, with the exception of the short time-scale perturbations caused by incomplete dispersion of bolus the SCR

model describes the data very well empirically. Second, the gamma variate fit would only be correct if the recirculating fraction of the tracer began only after the first pass of the bolus. In reality, recirculation will contribute some tracer to the circulation during the first pass.^{2,3} A simple gamma variate fit then overestimates the size of the bolus. In contrast, the SCR model provides a more realistic account of the contribution of recirculating tracer in the absence of tracer leakage, and there is some theoretical justification for describing recirculating contrast in this way.⁴ Finally, fitting the SCR model does not involve determining a last point to fit since it fits the entire CTC. This is particularly important since the choice of the last point is somewhat arbitrary and susceptible to noise but can nonetheless cause substantial errors in the fit.

In this study, we use computer simulation to investigate the effect on estimates of bolus area and first moment of fitting with the SCR and GV models with different methods of choosing the last fitting point.

II. METHODS

This retrospective study was approved by the Institutional Review Board of this institution. DSC data were acquired from 10 healthy subjects (six females and four males; age range 29–71, age mean and standard deviation 55.8 ± 13.9) at 3T using a gradient echo EPI sequence (60 images; TR 1s; TE 32 ms; FA 30°; matrix 128×128 ; FOV 230×230 mm²; 10×5 mm slices) during injection of 0.1 mmol/kg Gd-DTPA at a rate of 5 ml/s. All simulations were performed in MATLAB R2009b (Mathworks, Newton, MA).

A “noise free” signal time curve was first obtained from each subject by averaging brain signals over a single axial slice inferior to the ventricles. Vascular signals were excluded to eliminate distortions due to the nonlinearities in the relaxivity in pure blood. This was achieved by excluding pixels from the average where the signal drop was over 40% larger than the average signal drop over the entire brain. Fifteen different levels of Gaussian noise giving signal to noise ratios, SNRs, (defined as S_{pre}/σ where σ is the standard deviation of the prebolus signal, S_{pre}) from approximately 20–130 were applied to this “noise free” data. This process was repeated 200 times giving a total of 30,000 different simulated signals.

CTCs were modeled by both SCR and GV, converted to signal and fitted to the noisy signal data. Signal, S , was calculated using the standard expression

$$S = S_{pre} \exp(-rCT_E), \quad (3)$$

where S_{pre} is the prebolus signal, T_E is the echo time, r is the relaxivity, and C is concentration. Fitting to the signal is preferable because the weighting for each data point is equal for all signal intensities and because S_{pre} can be included as a fitting parameter, making optimum use of the available data in finding this parameter.

The last fitting point for the GV was determined using four methods (Fig. 1): (i) third time point after the bolus minimum,⁵ (ii) time point at half the bolus depth after the peak,⁶ (iii) an adaptive method using first time point after the bolus peak within one standard deviation of the post bolus signal, and (iv) visual determination.⁷ Figure 2 shows the noise free CTC (crosses), the bolus (solid line) and recirculation (dotted line) determined by the SCR fit and the bolus (dashed line) determined by a GV fit.

The different models were fitted using the alternate form of the gamma variate developed by Madsen.⁸ This form decouples gamma variate amplitude from the shape parameters and so gives more stable fits.

Next, for each fit the area under the curve (AUC) and the normalized first moment (FM) of the bolus (i.e., the gamma

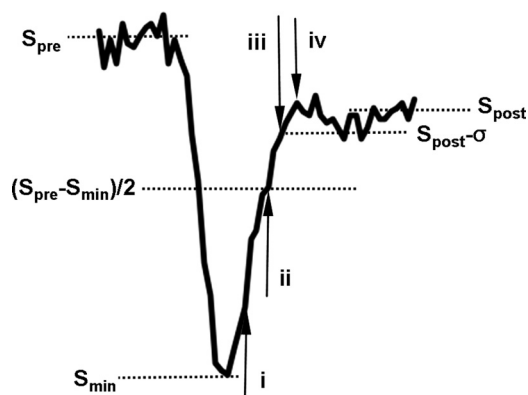


Fig. 1. Diagram of a typical signal time curve illustrating how the last fitted point for the gamma variate was selected for each method: (i) third point after the bolus minimum, (ii) point of the half drop of the bolus after the bolus minimum, (iii) the point after the minimum at which the signal exceeds the post bolus signal minus the standard deviation of the pre bolus signal (σ) and (iv) by visual determination.

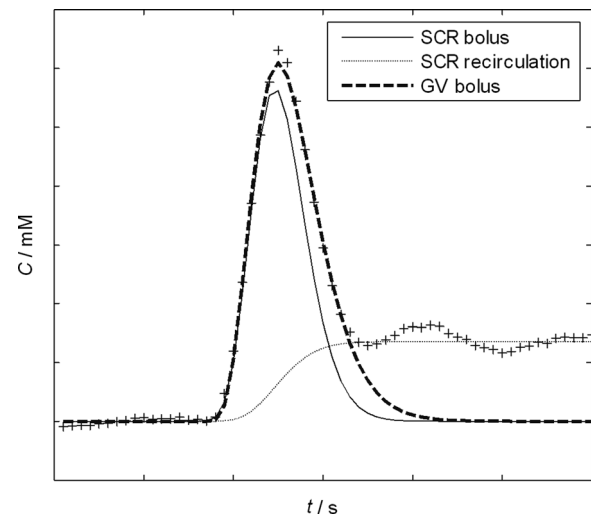


Fig. 2. Example of the bolus (solid line) and recirculation (dotted line) portions of the SCR model and bolus (dashed line) of a GV fitted to a typical concentration time curve (crosses).

variate portion of both SCR and GV models) were calculated using the following equations:

$$AUC = A \cdot C^{\beta+1} \cdot \Gamma(\beta + 1), \quad (4)$$

$$FM = C \cdot (\beta + 1) + t_0, \quad (5)$$

where Γ is the gamma function. CBV is proportional to AUC and CBF is a function of FM so these two parameters determine the errors that poor fits will introduce into perfusion estimates.

Finally, the percent error [Eq. (6)] and percent deviation [Eq. (7)] relative to values for the “noiseless” fit, respectively, were calculated

$$P.E._{SNR=i} = 100 \times \frac{|\bar{x} - x_{SNR=\infty}|}{x_{SNR=\infty}} \quad (6)$$

$$P.D._{SNR=i} = 100 \times \frac{\sqrt{\frac{1}{N} \sum (x - \bar{x})^2}}{\bar{x}} \quad (7)$$

where N is the number of trials.

III. RESULTS

Fitting proved to be extremely robust for both SCR and GV fits, even at low SNR. All 30,000 fits converged within the maximum allowed value of 200 iterations and most converged in less than 15. We did not observe any fits that appeared to have settled in false minima. The maximum, minimum, and median R^2 values were 0.99, 0.80, and 0.98, respectively.

Figure 3 shows typical fits for the SCR model [Figs. 3(a) and 3(b)] and for each GV method (i–iv) [Fig. 3(c)–3(j)] for the “noiseless” data and with noise added to reduce the SNR to 25.

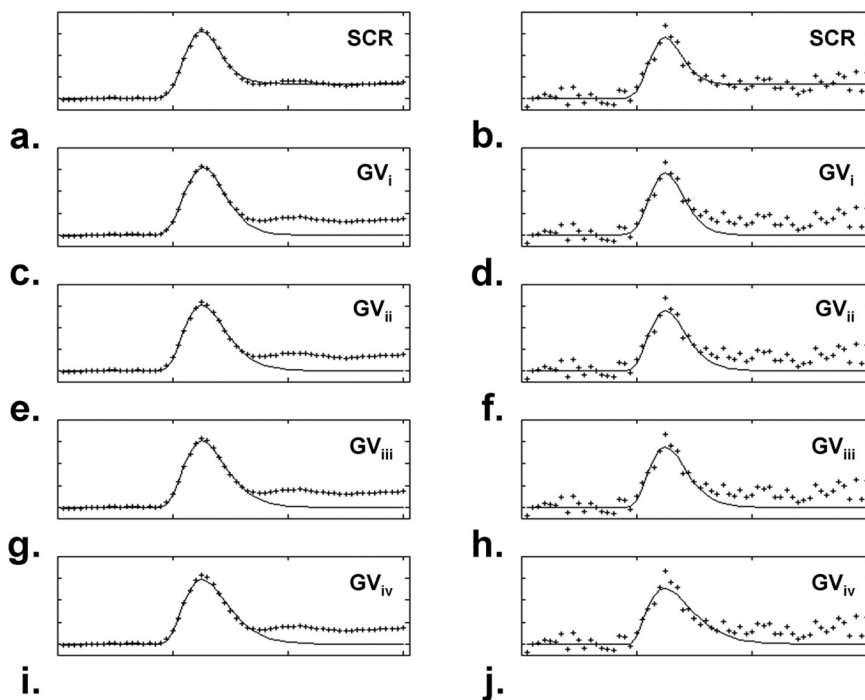


FIG. 3. Fits (line) to concentration time curves (crosses). The left column gives the “noiseless” concentration time curves and the right has added noise to give an SNR of 25.

The percent error and percent deviation of AUC [Figs. 4(a) and 4(b)] and FM [Figs. 4(c) and 4(d)] for the different models are plotted against SNR in Fig. 4. In general, GV_i (third point) performs poorly for both error and deviation. The SCR model, GV_{ii} (half depth) and GV_{iv} (visual inspection) give similar errors while GV_{iii} (adaptive) performs acceptably for AUC but poorly for FM. The SCR model performs as well as the best GV methods for AUC and rather better for FM.

Mean values of AUC and FM were smaller for the SCR model than values for all gamma variate fitting procedures as one would expect from Fig. 2. There were only small differences between mean values for the different GV methods. For example at an SNR of 100, SCR AUC and FM were 7.6 ± 1.73 AU and 8.8 ± 2.40 s, respectively, whereas GV values were 9.4 ± 1.88 AU and 10.0 ± 2.51 s.

IV. DISCUSSION

In this study, we compared the robustness with respect to noise of fitting arterial data with SCR and GV models with different methods of estimating the last point. Noise introduces both bias (i.e., systematic errors) and variability into AUC and FM estimates that will propagate to measurements of CBV, CBF, and mean transit time (MTT). CBV is proportional to the ratio of the AUCs measured in tissue and artery and it is typical to apply the model functions to both the arterial input function (AIF) and tissue measurements. The variance will be given by

$$\frac{\sigma_{CBV}}{CBV} = \sqrt{\left(\frac{\sigma_{A_T}}{A_T}\right)^2 + \left(\frac{\sigma_{A_A}}{A_A}\right)^2}, \quad (8)$$

where T and A_A are the AUCs in tissue and artery, respectively, and σ_{CBV} is the variance in CBV.

The relationship between FM and MTT is complex and, as far as we are aware cannot be expressed analytically. Overestimates of the MTT of the AIF due to errors will reduce estimated values of tissue MTT and hence increase estimates of CBF. Conversely overestimates of tissue MTT will lead to underestimates in CBF. Errors in CBV will also propagate to CBF. A full analysis is beyond the scope of this note.

Our results show that the SCR model is the most robust fitting technique with respect to noise both for bias and variability. The best of the gamma variate methods, GV_{iv} , produced similar or slightly worse results to the SCR model; however, the last point to fit in this method is determined visually. In this study, this was estimated from the “noise free” data since it is impractical to determine it in this way for 30,000 different data sets. However, this is a major practical disadvantage of this method. It is only feasible to apply this method on a pixel by pixel basis if it is assumed that the length of the bolus is the same for all pixels. Clearly, this is not the case and will result in significant errors.

The SCR model corrects for errors that are likely to be smaller than others often associated with DSC MRI. However, many of these errors can also be addressed effectively by improved processing and acquisition methods. For example, partial volume effects due to inadequate spatial resolution can be reduced using reference signals acquired from the sagittal sinus;⁹ signal “clipping” (saturation) can be reduced by reducing tracer dose or echo time; and the nonlinearity between relaxation and concentration can be addressed by using empirically derived calibration curves.¹⁰

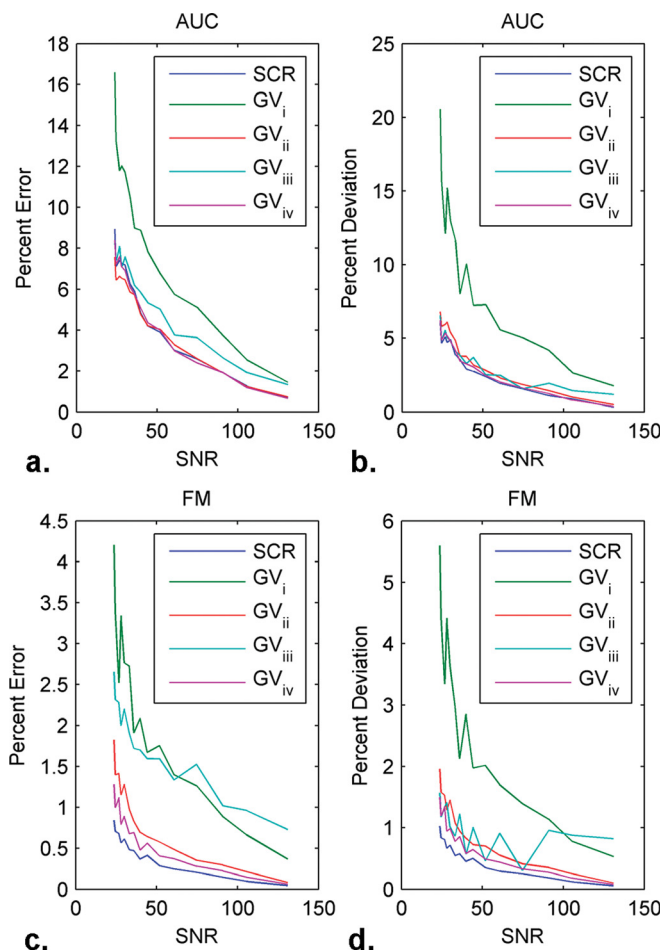


FIG. 4. Percent error (a) and percent deviation (b) of the AUC plotted against SNR for each model. Percent error (c) and percent deviation (d) of the FM plotted against SNR for each model.

There are a number of limitations of the SCR model and of this study. First, the model is based on the assumption that recirculation starts at the beginning of the bolus and increases as a gamma function. Neither of these assumptions can be fully justified. There may be a delay before recirculation contrast arrives and some other function may describe its arrival more accurately. Nonetheless the form of the function must be approximately sigmoidal similar to the form we suggest. Second, we did not consider the possible effects of cardiac output on our results. However, our subjects covered a wide age range (29–71) suggesting that cardiac output has relatively little effect. Third, the SCR model takes no account of errors introduced by incomplete dispersion leading to second or even third pass peaks. These errors might be particularly severe if too few measurements are taken after the bolus so

that the steady-state portion of the curve is not reached. We are currently investigating more sophisticated models that explicitly account for secondary peaks. Conversely, if too many data points are acquired after the bolus, the steady-state portion of the curve will start to decline because of tracer clearance through the kidneys. However, this can be accounted for by multiplying the SCR model by an exponential decay term. The model introduces one additional fitting parameter, λ , giving the possibility of over-fitting and instability. However, the effect of λ on the shape of the function is so different from those of the other parameters that this is not a serious risk in practice. Finally, the SCR model is subject to many of the same errors as the GV model such as tracer leakage, T1 contamination and partial volume effects.

In conclusion, we have demonstrated that the SCR model gives a more robust fit in the presence of noise while giving a more realistic representation of tracer boluses than the gamma variate.

ACKNOWLEDGEMENTS

This study was funded in part by NIH Grant No. R01CA111996.

- ^{a)} Author to whom correspondence should be addressed. Electronic mail: Vishal.Patil@nyumc.org. Telephone: (212) 263-8746.
- ¹ G. Johnson, S. G. Wetzel, S. Cha, J. Babb, and P. S. Tofts, "Measuring blood volume and vascular transfer constant from dynamic, T(2)*-weighted contrast-enhanced MRI," *Magn. Reson. Med.* **51**, 961–968 (2004).
- ² G. C. Sutton, J. Karnell, and G. Nylin, "Studies on the rapidity of complete blood circulation in man," *Am. Heart J.* **39**, 741–748 (1950).
- ³ C. W. Sheppard, *Basic Principles of the Tracer Method Introduction to Mathematical Tracer Kinetics* (John Wiley & Sons, Inc, New York, 1962).
- ⁴ N. A. Lassen and W. Perl, *Tracer Kinetic Methods in Medical Physiology* (Raven, New York, 1979).
- ⁵ A. A. Chan and A. J. Nelson, "Simplified gamma-variate fitting of perfusion curves," in *IEEE International Symposium on Biomedical Imaging: Nano to Macro* (IEEE, Arlington, VA, 2004), Vol. 2, pp. 1067–1070.
- ⁶ H. K. Thompson, Jr., C. F. Starmer, R. E. Whalen, and H. D. McIntosh, "Indicator Transit Time Considered as a Gamma Variate," *Circ. Res.* **14**, 502–515 (1964).
- ⁷ J. Perkio, H. J. Aronen, A. Kangasmaki, Y. Liu, J. Karonen, S. Savolainen, and L. Ostergaard, "Evaluation of four postprocessing methods for determination of cerebral blood volume and mean transit time by dynamic susceptibility contrast imaging," *Magn. Reson. Med.* **47**, 973–981 (2002).
- ⁸ M. T. Madsen, "A Simplified Formulation of the Gamma Variate Function," *Phys. Med. Biol.* **37**, 1597–1600 (1992).
- ⁹ W. Lin, A. Celik, C. Derdeyn, H. An, Y. Lee, T. Videen, L. Ostergaard, and W. J. Powers, "Quantitative measurements of cerebral blood flow in patients with unilateral carotid artery occlusion: A PET and MR study," *J. Magn. Reson. Imaging* **14**, 659–667 (2001).
- ¹⁰ E. Akbudak, M. S. Kotys, D. Memisevic, and T. E. Conturo, "Quadraticity and hematocrit dependence of $\Delta R2^*$ AIF signals at 3T: A blood phantom study under physiological conditions," in *Syllabus of the ISMRM workshop on Quantitative Cerebral Perfusion Imaging Using MRI: A Technical Perspective* (ISMRM, Venice, 2004), pp. 10–11.